Desalination and Water Treatment
www.deswater.com

doi: 10.1080/19443994.2015.1027276

57 (2016) 2446–2454
February

Taylor & Francis
Taylor & Francis Group

Production and characterization of activated carbons from pumpkin seed shell by chemical activation with $ZnCl_2$

İlknur Demiral*, Canan Aydın Şamdan, Hakan Demiral

Engineering and Architecture Faculty, Department of Chemical Engineering, Eskişehir Osmangazi University, Meşelik Campus, 26480 Eskişehir, Turkey, Tel. +90 222 239 3750/3663; Fax: +90 222 239 3613; email: idemiral@ogu.edu.tr (İ. Demiral)

Received 24 August 2014; Accepted 3 March 2015

ABSTRACT

In this study, an activated carbon with high surface area was prepared from pumpkin seed shell by chemical activation with $ZnCl_2$. The effects of impregnation ratio (IR) and activation temperature on the pore structure of the activated carbon were investigated. The activation temperatures and IRs were in the range of 400–600°C and 1:1–4:1, respectively. The chemical and physical properties of the obtained activated carbons were determined. Elemental analysis was applied to determine the C, H, N, and O contents, and Fourier transform infrared spectrophotometry was used to analyze the functional groups. The surface area, pore volumes, pore size distribution, and average pore diameter of the activated carbons were characterized by N_2 adsorption at 77 K using the Brunauer–Emmett–Teller (BET), *t*-plot, and density functional theory methods. The surface morphologies of the pumpkin seed shell and the activated carbon were investigated by scanning electron microscope. The highest BET surface area and total pore volume of the activated carbon were obtained as 1,564 m^2/g and 0.965 cm^3/g, respectively, at 500°C and with an IR of 3:1. According to the experimental results, pumpkin seed shell is a suitable raw material for activated carbon production.

Keywords: Activated carbon; Chemical activation; Characterization

1. Introduction

Activated carbons have been widely used as adsorbents in the separation and purification processes for gaseous or aqueous solution systems, and they are also used as catalysts or catalyst supports in the catalytic processes due to their large surface areas, microporous structures, high degree of surface reactivities, and high adsorption capacities [1–3]. Thus, activated carbons play an important role in the chemical, pharmaceutical, and food industries. Activated carbon can be produced theoretically from any carbonaceous material rich in elemental carbon. In activated carbons, the properties such as porosity, pore size distribution, pore shape, and surface chemistry are affected significantly by the nature of the precursor, activation method, and activation conditions [4]. In recent years, there has been considerable research concerning the preparation of low-cost activated carbons from different precursors such as walnut shell [5], cherry stones [6], pumpkin seed shell [7], palm shells [8], waste tea [9], orange skin [10], coconut shell [11], poplar wood [12], apricot stones [13], date pits, and rice husks [14].

*Corresponding author.

Presented at the 2nd International Conference on Recycling and Reuse (R&R2014), 4–6 June 2014, Istanbul, Turkey

Activated carbons can be produced basically by two methods: physical activation or chemical activation. In the physical activation, a raw material is first carbonized and the carbonized material is secondarily activated by steam or carbon dioxide, i.e. there are two steps: carbonization step and activation step [1]. In chemical activation, the raw material is first impregnated by activating reagents, such as H_3PO_4, $ZnCl_2$, K_2CO_3, NaOH, or KOH, followed by thermal activation under inert atmosphere to create the pore structure [15]. The carbonization step and the activation step simultaneously progress in the chemical activation. Chemical activation offers several advantages including activation in a single step, low activation temperatures, low activation time, and better porous structure [8,16]. On the other hand, there are some disadvantages of the chemical activation process such as the corrosiveness of the process and the necessity of washing steps [15].

Zinc chloride ($ZnCl_2$) is one of the most widely used agents for the chemical activation of a carbonaceous material. Chemical activation using zinc chloride produces high surface area and more porous activated carbons, and thus provides high adsorption capacity [5,17–20]. $ZnCl_2$ acts as a dehydrating agent promoting the decomposition of carbonaceous material during the pyrolysis process, restricts the formation of tar, and increases the carbon yield. Due to these properties, $ZnCl_2$ was selected as an activating agent.

The aim of this study was to obtain a useful activated carbon by evaluating waste pumpkin seed shells. In the study, activated carbons were produced from pumpkin seed shell by chemical activation with zinc chloride. The effects of carbonization temperature and impregnation ratio (IR) on the pore structure (specific surface area, pore volume, and pore size distribution) were investigated by N_2 adsorption.

In addition, the prepared activated carbons were characterized by several techniques such as elemental analysis, Fourier transform infrared (FTIR), and scanning electron microscope (SEM). Functional groups are very important characteristics of the activated carbons, since they determine the surface properties of the carbons and their quality. The FTIR spectroscopy in its various forms is an important and forceful technique which can give useful information about structures. Surface morphology of the pumpkin seed shell and the activated carbon was investigated by SEM.

2. Experimental

2.1. The material

The pumpkin seed shell used in this study was the pumpkin seed process waste of Peyman Company which produces all kinds of nuts and dried fruits in Eskişehir. The dried sample at 105°C was crushed and sieved to obtain a 0.850 –1.00 mm grain size by a high-speed rotary cutting mill.

2.2. Preparation of activated carbons

In this study, the chemical activation of pumpkin seed shell was carried out using zinc chloride ($ZnCl_2$). The IR was calculated as the ratio of the weight of $ZnCl_2$ in solution to the weight of the used pumpkin seed shell. The IR was varied between 1:1 and 4:1. Twenty to eighty grams of $ZnCl_2$ were dissolved in 200 mL of distilled water, and then 20 g of the pumpkin seed shells were mixed with the $ZnCl_2$ solution and stirred at approximately 75°C for 6 h to ensure a complete reaction between $ZnCl_2$ and pumpkin seed shell particles. The mixtures were then filtered and the remaining solids were dried at 105°C for about 24 h.

The impregnated pumpkin seed shell was placed in a vertical tree zone tubular furnace (Carbolite, UK). The heated length is divided into three zones. The outer diameter of the tube is 75 mm, and the maximum operating temperature is 1,200°C.

The impregnated pumpkin seed shell was carbonized at the desired temperatures (400, 500, and 600°C) under nitrogen flow. The carbonization process was initiated by heating the sample with a heating rate of 10°C/min starting from room temperature until the desired temperature was reached. The samples were held at the desired temperature for 1 h. Then, the temperature of the reactor was cooled down to the room temperature under nitrogen atmosphere. The activated carbons were washed with a 0.5 N HCl solution. Subsequently, the samples were repeatedly washed with hot distilled water until the pH of the solution reached a value between 6 and 7. Finally, the wet samples were dried at 105°C for 24 h and weighed to calculate the yield. The activated carbon yield was calculated by the following equation:

$$\text{Yield of activated carbon (wt\%)} = \frac{\text{Final weight of activated carbon}}{\text{Initial weight of pumpkin seed shell}} \times 100 \quad (1)$$

2.3. Characterization of the activated carbons

The carbon, hydrogen, nitrogen, and oxygen (by difference) contents of the pumpkin seed shell and activated carbons were measured using a LECO, CHNS-932 model Elemental Analyzer.

The determination of the porosity of activated carbon samples was performed using physical adsorption of N_2 at 77 K (Quantachrome, Autosorb-1C). The surface area, pore volume, and pore size distribution were determined from nitrogen adsorption data by using Quantachrome software. Prior to gas adsorption measurements, the samples were degassed at 300˚C under vacuum for 3 h. The adsorption data were obtained in a relative pressure, P/P^o, range of 10^{-5} to 1. The Brunauer–Emmett–Teller (BET) surface area was calculated from N_2 adsorption isotherms by using the BET equation within the 0.01–0.15 relative pressure range [21]. The *t*-plot method was applied to calculate the micropore volume [22]. The total pore volumes were calculated at a relative pressure of 0.995. The pore size distributions of the activated carbons were determined by density functional theory method [23].

The functional groups on the surface of the activated carbon were determined by Perkin Elmer 100 Model FTIR spectrophotometer. The spectrum was obtained over the range of 400–4,000 cm^{-1}. The surface morphologies were studied by SEM. The SEM images were obtained using JEOL-JSM-5600LV SEM.

3. Results and discussion

Table 1 shows the ultimate and proximate analysis results of the precursor. A high carbon and low ash content of pumpkin seed shell indicates that the precursor is suitable for activated carbon production.

3.1. Yield of activated carbon

The yield of activated carbon was calculated from the weight of the resultant activated carbons divided by the weight of dried pumpkin seed shell. The effects of activation temperature and IR are shown in Fig. 1.

The final activation temperature and IR play an important role on the yield of activated carbon. It can be seen from Fig. 1 that as the activation temperature increases from 400 to 600˚C, the percentage yield decreases for all IRs. This is due to the loss of the volatile materials with increasing temperature [24,25]. On the other hand, at each activation temperature, the activated carbon yields decreased with increasing IR. As the IR increases, the percentage yield of the activated carbon decreases gradually due to the continuous removal of tar material from the pores. Ahmed and Theydan obtained similar results for the activation of date stones under operating conditions similar to those applied in this work [16].

Table 1
Proximate and ultimate analyses (wt.%) of pumpkin seed shell

Characteristics	Percentage (wt.%)
Proximate analysis	
Moisture content	7.60
Volatiles	70.97
Ash	3.90
Fixed carbon[a]	17.53
Ultimate analysis	
Carbon	48.79
Hydrogen	7.52
Nitrogen	3.97
Oxygen[a]	39.72

[a]By difference.

3.2. Elemental analysis of the produced activated carbon

The elemental analysis results of the activated carbons obtained at various activation temperatures and IRs are shown in Table 2. Compared to the pumpkin seed shell, all carbon samples had higher contents of C and lower contents of H and O. It can be said that chemical activation accelerated the removal of H and O and this resulted in an increased C content as expected.

As can be seen from Table 2, with an increase in the activation temperatures from 400 to 600˚C, the carbon content of the activated carbon samples increased from 68.86 to 76.45 wt.%. However, the hydrogen content decreased from 3.87 to 2.82 wt.%, and the oxygen content also showed a similar trend, decreasing from 24.42 to 18.02 wt.%, for the IR of 3:1. The effects of the IRs on the elemental compositions of the activated carbon samples were similar for 500˚C. The carbon contents of the activated carbon samples obtained for

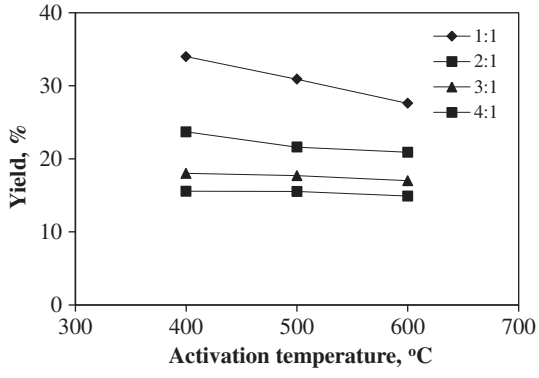

Fig. 1. Effect of the activation temperature and IR on the yield of activated carbons.

Table 2
Elemental analyses of activated carbons produced at different activation temperatures and IRs

$ZnCl_2$ impregnation ratio: 3:1 Activation temperature (°C)	wt.%			
	Carbon	Hydrogen	Nitrogen	Oxygen*
400	68.86	3.87	2.85	24.42
500	75.71	3.07	2.70	18.52
600	76.45	2.82	2.71	18.02
Activation temperature: 500°C				
Impregnation ratio				
1:1	54.97	2.84	3.38	38.81
2:1	68.69	3.76	2.75	24.80
3:1	75.71	3.07	2.70	18.52
4:1	76.81	2.61	2.64	17.94

*By difference.

various activation conditions were increased compared to pumpkin seed shell. This is due to the release of volatiles during carbonization that resulted in the elimination of non-carbonaceous parts and enrichment of carbon [26]. The variation of the elemental analysis was found to follow a similar trend in activated carbons produced from other precursors such as waste tea, nutshells, fibrous textile waste, cherry stones, and kraft lignin [20,26–29].

3.3. Surface area and pore size distribution

The adsorption behavior and pore structure of the activated carbons can be analyzed using nitrogen adsorption isotherms. General properties of activated carbons can be explained by the shape of these isotherms [24]. The N_2 adsorption–desorption isotherms of the activated carbons obtained at different temperatures are shown in Fig. 2. From the shape of the isotherms, it may be stated that all activated carbons exhibit Type I isotherms with an almost horizontal plateau at higher relative pressures, indicating highly microporous materials. However, the small hysteresis loops seen on the adsorption–desorption isotherms of the activated carbons are due to the existence of mesopores [30]. The major uptake occurs at relative pressure less than 0.1. The initial part of the isotherm represents micropore filling, and a low slope of the plateau indicates multilayer adsorption on the external surface.

Surface properties of the activated carbons prepared at different temperatures and IRs are shown in Table 3.

The effect of activation temperature on the surface area and total pore volume was evaluated at the IR of

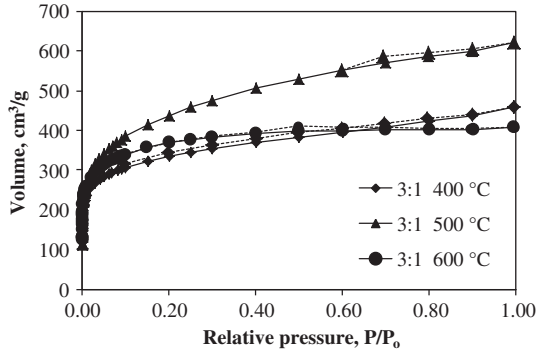

Fig. 2. Adsorption–desorption isotherms of the activated carbons (IR = 3:1) (the dotted lines (- - - - -) represent desorption isotherms).

3:1. The surface area increased from 1,148 to 1,564 m^2/g, as the temperature was increased from 400 to 500°C and then decreased to 1,369 m^2/g at 600°C. The total pore volume followed the same trend. The BET surface areas and total pore volumes of the samples reach their maximum values at a temperature of 500°C. Above 500°C, pore widening causes collapse of pore volumes, and surface area and pore volumes begin to decrease. This indicates that pore formation is affected by both the reaction between incorporated $ZnCl_2$ and the precursor, and thermal pyrolysis of the precursor [30]. Similar results were obtained by other researchers [31,32].

The surface areas and pore volumes of the activated carbons prepared at 500°C activation temperature using various IRs are shown in Table 3. The BET surface area and total pore volume of the activated carbon increased from 841 to 1,564 m^2/g and from

Table 3
Surface properties of the activated carbons

Impregnation ratio (wt/wt)	Activation temperature (°C)	S_{BET} (m^2/g)	V_{mic} (cm^3/g)	V_{tot} (cm^3/g)	D_p (Å)
1:1	500	841	0.246	0.483	22.97
2:1	500	1,374	0.516	0.654	23.15
3.1	400	1,148	0.408	0.649	23.85
3:1	500	1,564	0.526	0.965	24.69
3:1	600	1,369	0.547	0.633	18.31
4:1	500	1,395	0.438	0.851	26.42

0.483 to 0.965 cm^3/g, respectively, as the IR increased from 1:1 to 3:1. An increase in the amount of activating agent promotes the contact area between pumpkin seed shell and activating agent, which promotes the diffusion of $ZnCl_2$ into the structure. This leads finally to an increase in the porosity. However, the surface area and total pore volume of the activated carbon decreased to 1,395 m^2/g and 0.851 cm^3/g, respectively, as the IR increased from 3:1 to 4:1. When the IR increased from 3:1 to 4:1, new micropores did not grow any longer, while existing micropores were continuously enlarged into mesopores, resulting in decrease in V_{mic}. Similar results were obtained by other researchers [20,24,33].

A comparison of the surface areas of other activated carbons derived from different precursors in the literature was given in Table 4. The activated carbon prepared in this work showed relatively high S_{BET} of 1,564 m^2/g, as compared to some previous works reported in the literature.

The pore size distribution of the activated carbons produced from pumpkin seed shell at various activation temperatures in the IR of 3:1 is given in Fig. 3. Porous structure of activated carbons contains a wide range of pore sizes. For practical reasons, they are classified into three groups: micropore (pore size <2 nm), mesopore (2–50 nm), and macropore (>50 nm) by the International Union of Pure and Applied Chemistry [4,45]. Micropores can be divided into ultramicropores (width less than 0.7 nm) and supermicropores (width from 0.7 to 2 nm) [46]. All activated carbons produced from pumpkin seed shell in this study include both micropores and mesopores. However, the micropore volumes are larger than mesopore volumes for all carbons. The average pore diameters of the activated carbons between 18.31 and 26.42 Å principally denoted microporous and mesoporous characteristics. Similar results were obtained for the activated carbons produced from waste tea, cherry stones, cattle-manure compost, and olive bagasse [20,33,47].

Table 4
Comparison of the surface areas of activated carbons derived from different precursors

Precursors	Activating agent	Impregnation ratio	Activation temperature (°C)	S_{BET} (m^2/g)	References
Pumpkin seed shell	$ZnCl_2$	3	500	1,564	This study
Grape seed	H_3PO_4	3	500	1,139	[34]
Olive tree wood	H_3PO_4	3.5	550	904	[35]
Cherry stones	$ZnCl_2$	3	700	1,704	[36]
Rice husk	H_3PO_4	4	500	1,543	[37]
Rice husk	KOH	4	800	2,516	[37]
Walnut shell	$ZnCl_2$	2	450	800	[5]
Cotton stalk	H_3PO_4	3	500	1,160	[38]
Sewage sludge	KOH	3	750	1,832	[39]
Apple pulp	$ZnCl_2$	1	500	1,067	[40]
Jatropha curcas seeds	NaOH	–	800	1,758	[41]
Paulownia wood	$ZnCl_2$	4	400	2,736	[42]
Sugar beet bagasse	$ZnCl_2$	3	700	1,826	[43]
Grape stalk	$ZnCl_2$	2	700	1,411	[44]
Palm shell	H_3PO_4	3	425	1,109	[8]

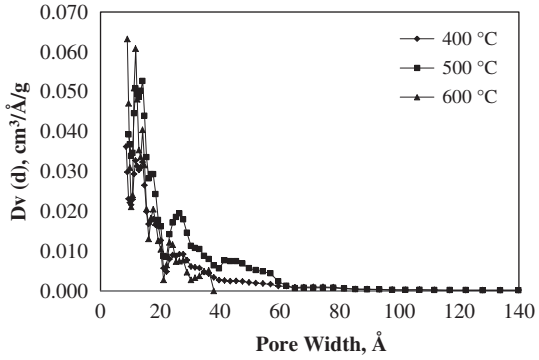

Fig. 3. Pore size distribution of prepared activated carbons with variable temperature (IR = 3:1).

3.4. SEM analyses

SEM technique was used to observe the surface physical morphology of the samples. Fig. 4 illustrates the SEM photographs of pumpkin seed shell and activated carbon obtained at activation temperature of 500˚C and IR of 3:1. The morphology of the activated carbon differs from that of the pumpkin seed shell. The surface of the pumpkin seed shell was quite smooth without any porous structure except for some occasional cracks, as supported by the BET results (7.96 m^2/g). On the contrary, the activated carbon has remarkable well-developed pore structure indicative of a high surface area. It can be seen from the SEM images that the external surface of the $ZnCl_2$-activated carbon is full of cavities, and the pores have different sizes and different shapes [48]. It seems that the cavities on the surface of the carbon resulted from the evaporation of $ZnCl_2$ during carbonization, leaving the space previously occupied by the $ZnCl_2$ [20,49]. Therefore, the $ZnCl_2$ is an effective activating agent to obtain activated carbon having high surface area.

3.5. FTIR analyses

Functional groups are very important characteristics of the activated carbons, since they determine the surface properties of the carbons and their quality. The FTIR spectroscopy in its various forms is an important and forceful technique which can give useful information about structures. It can provide basic spectra of activated carbons, especially for determination of types and intensities of their surface functional groups [50]. FTIR analysis results of pumpkin seed shell and activated carbon (IR = 3:1, 500˚C) are given in Fig. 5.

The spectrum of the derived activated carbon is different from that of the raw material. Many bands disappeared or weakened during the activated carbon preparation including the impregnation and the activation; in particular, the bands located in two regions between 3,600 and 2,800 cm^{-1} and between 800 and 400 cm^{-1} [38]. The first peak at 3,300 cm^{-1} is ascribed to OH stretching vibration in hydroxyl groups. This peak is stronger for the pumpkin seed shell and has weakened for the activated carbon [27]. Two strong bands observed at 2,920 and 2,860 cm^{-1} are assigned to asymmetric C–H and symmetric C–H bands, respectively, present in alkyl groups such as methyl and methylene groups [51]. However, this band disappeared in the activated carbon. These bands were visible in raw material, but not in activated carbon. The strong band is seen at about 1,638 cm^{-1} that may be ascribed to olefinic C=C vibrations in aromatic region for the raw material [27]. Another strong band at 1,030 cm^{-1} represents C–O stretching vibrations in the raw material.

The spectra of the prepared activated carbon also show a strong band at 1,600–1,580 cm^{-1} due to C–C vibrations in aromatic rings [52,53]. The peaks between 1,050 and 1,350 cm^{-1} occurred due to the

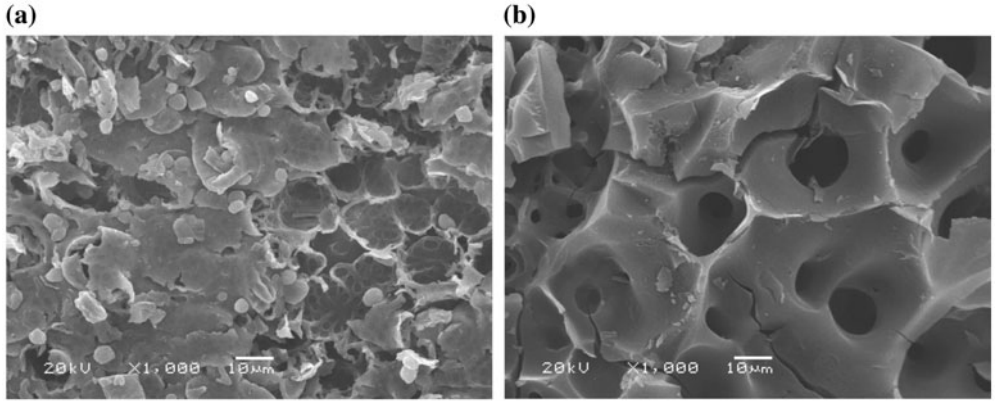

Fig. 4. SEM images of (a) pumpkin seed shell and (b) activated carbon.

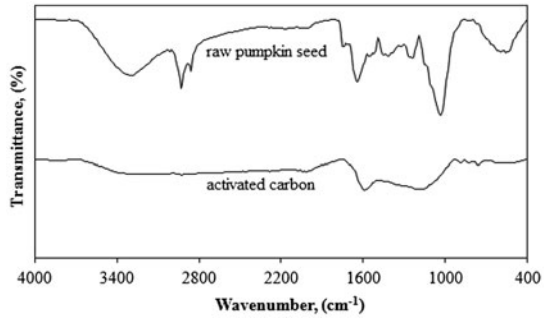

Fig. 5. FTIR spectra.

presence of primary, secondary, and tertiary alcohols, phenols, ethers, and esters showing C–O stretching and O–H deformation vibrations in activated carbon.

4. Conclusion

Pumpkin seed shell was used as a raw material to prepare activated carbons by chemical activation method with $ZnCl_2$. The effects of activation temperature and IR on the pore structure and surface chemistry of the activated carbons were investigated. The BET surface areas and total pore volumes of the obtained activated carbons produced from pumpkin seed shell have a high surface area and a highly developed micropore structure. The maximum surface area and pore volume were obtained at the IR of 3:1 and the carbonization temperature of 500˚C. The maximum BET surface area and total pore volume were determined as 1,564 m^2/g and 0.965 cm^3/g, respectively. The pore size distribution shows that the activated carbons include both micropores and mesopores. The surface morphologies of the raw material and the activated carbon were investigated by SEM analysis. The SEM images show the effect of $ZnCl_2$ activation on the pore development.

According to the results of this study, it can be said that the pumpkin seed shell can be effectively used as a raw material for the preparation of activated carbon using chemical activation procedure. The activated carbon produced from an agricultural waste with high carbon content is one of the most important materials to eliminate environmental pollution (gases and liquid impurities). Various activated carbons produced from agricultural wastes were reported for the removal of pollutants such as Cr(VI) (longan seed activated carbon S_{BET} = 1,511 m^2/g) [54], basic dyes (methylene blue and rhodamine B) (orange peel activated carbon S_{BET} = 1,090 m^2/g) [55], cadmium (bamboo activated carbon S_{BET} = 608 m^2/g) [56], and copper (cassava peel activated carbon S_{BET} = 1,567 m^2/g) [57].

As a result, the activated carbon product with high surface area obtained in this study can be used as an adsorbent for various environmental applications including the removal of organic and inorganic hazardous compounds from industrial gases or aqueous solutions for the purification or the recovery of chemicals.

Acknowledgment

This study was financially supported by Eskişehir Osmangazi University Scientific Research Foundation (Project No: 201315A103).

References

[1] J. Hayashi, T. Horikawa, I. Takeda, K. Muroyama, F.N. Ani, Preparing activated carbon from various nutshells by chemical activation with K_2CO_3, Carbon 40 (2002) 2381–2386.
[2] T.M. Alslaibi, I. Abustan, M.A. Ahmad, A.A. Foul, Cadmium removal from aqueous solution using microwaved olive stone activated carbon, J. Environ. Chem. Eng. 1 (2013) 589–599.
[3] S.Z. Mohammadi, M.A. Karimi, D. Afzali, F. Mansouri, Removal of Pb(II) from aqueous solutions using activated carbon from sea-buckthorn stones by chemical activation, Desalination 262 (2010) 86–93.
[4] Ç. Şentorun-Shalaby, M.G. Uçak-Astarlıoğlu, L. Artok, Ç. Sarıcı, Preparation and characterization of activated carbons by one-step steam pyrolysis/activation from apricot stones, Micropor. Mesopor. Mater. 88 (2006) 126–134.
[5] J. Yang, K. Qiu, Preparation of activated carbons from walnut shells via vacuum chemical activation and their application for methylene blue removal, Chem. Eng. J. 165 (2010) 209–217.
[6] M. Olivares-Marin, C. Fernandez-Gonzalez, A. Macias-Garcia, V. Gomez-Serrano, Preparation of activated carbon from cherry stones by physical activation in air. Influence of the chemical carbonisation with H_2SO_4, J. Anal. Appl. Pyrolysis 94 (2012) 131–137.
[7] A.I. Okoye, P.M. Ejikeme, O.D. Onukwuli, Lead removal from wastewater using fluted pumpkin seed shell activated carbon: Adsorption modeling and kinetics, Int. J. Environ. Sci. Technol. 7 (2010) 793–800.
[8] W.C. Lim, C. Srinivasakannan, N. Balasubramanian, Activation of palm shells by phosphoric acid impregnation for high yielding activated carbon, J. Anal. Appl. Pyrolysis 88 (2010) 181–186.
[9] I.I. Gurten, M. Ozmak, E. Yağmur, Z. Aktaş, Preparation and characterisation of activated carbon from waste tea using K_2CO_3, Biomass Bioenerg. 37 (2012) 73–81.
[10] J.M. Rosas, J. Bedia, J. Rodriquez-Mirasol, T. Cordero, On the preparation and characterization of chars and activated carbons from orange skin, Fuel Process. Technol. 91 (2010) 1345–1354.

[11] A.L. Cazetta, A.M.M. Vargas, E.M. Nogami, M.H. Kunita, M.R. Guilherme, A.C. Martins, T.L. Silva, J.C.G. Moraes, V.C. Almeida, NaOH-activated carbon of high surface area produced from coconut shell: Kinetics and equilibrium studies from the methylene blue adsorption, Chem. Eng. J. 174 (2011) 117–125.
[12] H. Demiral, I. Uzun, Preparation and characterization of activated carbons from poplar wood (Populus L.), Surf. Interface Anal. 42 (2010) 1338–1341.
[13] K. Belaroui, A. Seghier, M. Hadjel, Synthesis of activated carbon based on apricot stones for wastewater treatment, Desalin. Water Treat. 52 (2014) 1422–1433.
[14] F.M.S.E. El-Dars, M.A. Ibrahim, A.M.E. Gabr, Reduction of COD in water-based paint wastewater using three types of activated carbon, Desalin Water Treat. 52 (2014) 2975–2986.
[15] S. Timur, İ.C. Kantarlı, S. Onenc, J. Yanik, Characterization and application of activated carbon produced from oak cups pulp, J. Anal. Appl. Pyrolysis 89 (2010) 129–136.
[16] M.J. Ahmed, S.K. Theydan, Physical and chemical characteristics of activated carbon prepared by pyrolysis of chemically treated date stones and its ability to adsorb organics, Powder Technol. 229 (2012) 237–245.
[17] F. Boudrahem, F. Aissani-Benissad, H. Ait-Amar, Batch sorption dynamics and equilibrium for the removal of lead ions from aqueous phase using activated carbon developed from coffee residue activated with zinc chloride, J. Environ. Manage. 90 (2009) 3031–3039.
[18] M. İmamoğlu, O. Tekir, Removal of copper (II) and lead (II) ions from aqueous solutions by adsorption on activated carbon from a new precursor hazelnut husks, Desalination 228 (2008) 108–113.
[19] M. Kılıç, E. Apaydın-Varol, A. Eren Pütün, Preparation and surface characterization of activated carbons from *Euphorbia rigida* by chemical activation with $ZnCl_2$, K_2CO_3, NaOH and H_3PO_4, Appl. Surf. Sci. 261 (2012) 247–254.
[20] D. Angın, Production and characterization of activated carbon from sour cherry stones by zinc chloride, Fuel 115 (2014) 804–811.
[21] G.G. Stavropoulos, A.A. Zabaniotou, Production and characterization of activated carbons from olive-seed waste residue, Micropor. Mesopor. Mater. 82 (2005) 79–85.
[22] Y. Önal, C. Akmil-Başar, Ç. Sarıcı-Özdemir, S. Erdoğan, Textural development of sugar beet bagasse activated with $ZnCl_2$, J. Hazard. Mater. 142 (2007) 138–143.
[23] Y. Sudaryanto, S.B. Hartono, W. Irawaty, H. Hindarso, S. Ismadji, High surface area activated carbon prepared from cassava peel by chemical activation, Bioresour. Technol. 97 (2006) 734–739.
[24] T.C. Chandra, M.M. Mirna, J. Sunarso, Y. Sudaryanto, S. Ismadji, Activated carbon from durian shell: Preparation and characterization, J. Taiwan Inst. Chem. Eng. 40 (2009) 457–462.
[25] C. Bouchelta, M.S. Medjram, O. Bertrand, J.P. Bellat, Preparation and characterization of activated carbon from date stones by physical activation with steam, J. Anal. Appl. Pyrolysis 82 (2008) 70–77.
[26] A. Aygün, S. Yenisoy-Karakaş, I. Duman, Production of granular activated carbon from fruit stones and nutshells and evaluation of their physical, chemical and adsorption properties, Micropor. Mesopor. Mater. 66 (2003) 189–195.
[27] E. Yağmur, M. Ozmak, Z. Aktaş, A novel method for production of activated carbon from waste tea by chemical activation with microwave energy, Fuel 87 (2008) 3278–3285.
[28] P.T. Williams, A.R. Reed, High grade activated carbon matting derived from the chemical activation and pyrolysis of natural fibre textile waste, J. Anal. Appl. Pyrolysis 71 (2004) 971–986.
[29] V. Fierro, V. Torne-Fernandez, A. Celzard, Kraft lignin as a precursor for microporous activated carbons prepared by impregnation with ortho-phosphoric acid: Synthesis and textural characterisation, Micropor. Mesopor. Mater. 92 (2006) 243–250.
[30] Y. Guo, D.A. Rockstraw, Activated carbons prepared from rice hull by one-step phosphoric acid activation, Micropor. Mesopor. Mater. 100 (2007) 12–19.
[31] J. Hayashi, A. Kazehaya, K. Muroyama, A.P. Watkinson, Preparation of activated carbon from lignin by chemical activation, Carbon 38 (2000) 1873–1878.
[32] L.Y. Hsu, H. Teng, Influence of different chemical reagents on the preparation of activated carbons from bituminous coal, Fuel Process. Technol. 64 (2000) 155–166.
[33] Q. Qian, M. Machida, H. Tatsumoto, Preparation of activated carbons from cattle-manure compost by zinc chloride activation, Bioresour. Technol. 98 (2007) 353–360.
[34] M. Al Bahri, L. Calvo, M.A. Gilarranz, J.J. Rodriguez, Activated carbon from grape seeds upon chemical activation with phosphoric acid: Application to the adsorption of diuron from water, Chem. Eng. J. 203 (2012) 348–356.
[35] A. Ould-Idriss, M. Stitou, E.M. Cuerda-Correa, C. Fernandez-Gonzalez, A. Macias-Garcia, M.F. Alexandre-Franco, V. Gomez-Serrano, Preparation of activated carbons from olive-tree wood revisited. I.Chemical activation with H_3PO_4, Fuel Process. Technol. 92 (2011) 261–265.
[36] D. Angın, Utilization of activated carbon produced from fruit juice industry solid waste for the adsorption of Yellow 18 from aqueous solutions, Bioresour. Technol. 168 (2014) 259–266.
[37] L. Ding, B. Zou, W. Gao, Q. Liu, Z. Wang, Y. Guo, X. Wang, Y. Liu, Adsorption of Rhodamine-B from aqueous solution using treated rice husk-based activated carbon, Colloids Surf., A 446 (2014) 1–7.
[38] M.A. Nahil, P.T. Williams, Pore characteristics of activated carbons from the phosphoric acid chemical activation of cotton stalks, Biomass Bioenerg. 37 (2012) 142–149.
[39] V.M. Monsalvo, A.F. Mohedano, J.J. Rodriguez, Activated carbons from sewage sludge application to aqueous-phase adsorption of 4-chlorophenol, Desalination 277 (2011) 377–382.
[40] T. Depci, A.R. Kul, Y. Önal, Competitive adsorption of lead and zinc from aqueous solution on activated carbon prepared from Van apple pulp: Study in single- and multi-solute systems, Chem. Eng. J. 200–202 (2012) 224–236.

[41] S.H. Hsu, C.S. Huang, T.W. Chung, S. Gao, Adsorption of chlorinated volatile organic compounds using activated carbon made from *Jatropha curcas* seeds, J. Taiwan Inst. Chem. Eng. 45 (2014) 2526–2530.
[42] S. Yorgun, N. Vural, H. Demiral, Preparation of high-surface area activated carbons from Paulownia wood by $ZnCl_2$ activation, Micropor. Mesopor. Mater. 122 (2009) 189–194.
[43] H. Demiral, G. Gündüzoğlu, Removal of nitrate from aqueous solutions by activated carbon prepared from sugar beet bagasse, Bioresour. Technol. 101 (2010) 1675–1680.
[44] I. Özdemir, M. Şahin, R. Orhan, M. Erdem, Preparation and characterization of activated carbon from grape stalk by zinc chloride activation, Chem. Eng. J. 158 (2010) 129–142.
[45] A. Namane, A. Mekarzıa, K. Benrachedi, N. Belhaneche-Bensemra, A. Helall, Determination of the adsorption capacity of activated carbon made from coffee grounds by chemical activation with $ZnCl_2$ and H_3PO_4, J. Hazard. Mater. 119 (2005) 189–194.
[46] W. Li, L. Zhang, J. Peng, N. Li, X. Zhu, Preparation of high surface area activated carbons from tobacco stems with K_2CO_3 activation using microwave radiation, Ind. Crops Prod. 27 (2008) 341–347.
[47] M. Olivares-Marin, C. Fernandez-Gonzalez, A. Macias-Garcia, V. Gomez-Serrano, Preparation of activated carbon from cherry stones by chemical activation with $ZnCl_2$, Appl. Surf. Sci. 252 (2006) 5967–5971.
[48] K. Li, Z. Zheng, Y. Li, Characterization and lead adsorption properties of activated carbons prepared from cotton stalk by one-step H_3PO_4 activation, J. Hazard. Mater. 181 (2010) 440–447.
[49] H. Demiral, İ. Demiral, Surface properties of activated carbon prepared from wastes, Surf. Interface Anal. 40 (2008) 612–615.
[50] M.Ö. Abdullah, I.A.W. Tan, L.S. Lim, Automobile adsorption air-conditioning system using oil palm biomass-based activated carbon: A review, Renew. Sust. Energ. Rev. 15 (2011) 2061–2072.
[51] A.A. El-Hendawy, Variation in the FTIR spectra of a biomass under impregnation, carbonization and oxidation conditions, J. Anal. Appl. Pyrolysis 75 (2006) 159–166.
[52] M. Benadjemia, L. Millirre, L. Reinert, N. Benderdouche, L. Duclaux, Preparation, characterization and Methylene Blue adsorption of phosphoric acid activated carbons from globe artichoke leaves, Fuel Process. Technol. 92 (2011) 1203–1212.
[53] C. Saka, BET, TG–DTG, FT-IR, SEM, iodine number analysis and preparation of activated carbon from acorn shell by chemical activation with $ZnCl_2$, J. Anal. Appl. Pyrolysis 95 (2012) 21–24.
[54] J. Yang, M. Yu, W. Chen, Adsorption of hexavalent chromium from aqueous solution by activated carbon prepared from longan seed: Kinetics, equilibrium and thermodynamics, J. Ind. Eng. Chem. 21 (2015) 414–422.
[55] M.E. Fernandez, G.V. Nunell, P.R. Boneli, A.L. Cukierman, Activated carbon developed from orange peels: Batch and dynamic competitive adsorption of basic dyes, Ind. Crops Prod. 62 (2014) 437–445.
[56] P.G. Gonzalez, Y.B. Pliego-Cuervo, Adsorption of Cd (II), Hg(II) and Zn(II) from aqueous solution using mesoporous activated carbon produced from *Bambusa vulgaris* striata, Chem. Eng. Res. Des. 92 (2014) 2715–2724.
[57] J.C. Moreno-Pirajan, L. Giraldo, Adsorption of copper from aqueous solution by activated carbons obtained by pyrolysis of cassava peel, J. Anal. Appl. Pyrolysis 87 (2010) 188–193.